

Comparative tissue transcriptomics highlights dynamic differences among tissues but conserved metabolic transcript prioritization in preparation for arousal from torpor

Lori K. Bogren¹ · Katharine R. Grabek² · Gregory S. Barsh³ · Sandra L. Martin¹

Received: 1 September 2016 / Revised: 2 November 2016 / Accepted: 26 February 2017 / Published online: 23 March 2017
© Springer-Verlag Berlin Heidelberg 2017

Abstract During the hibernation season, 13-lined ground squirrels spend days to weeks in torpor with body temperatures near freezing then spontaneously rewarm. The molecular drivers of the drastic physiological changes that orchestrate and permit torpor are not well understood. Although transcription effectively ceases at the low body temperatures of torpor, previous work has demonstrated that some transcripts are protected from bulk degradation in brown adipose tissue (BAT), consistent with the importance of their protein products for metabolic heat generation during arousal from torpor. We examined the transcriptome of skeletal muscle, heart, and liver to determine the patterns of differentially expressed genes in these tissues, and whether, like BAT, a subset of these were relatively increased during torpor. EDGE-tags were quantified from five distinct physiological states representing the seasonal and torpor-arousal cycles of 13-lined ground squirrels. Supervised clustering on relative transcript abundances with Random Forest separated the two states bracketing

prolonged torpor, entrance into and aroused from torpor, in all three tissues. Independent analyses identified 3347, 6784, and 2433 differentially expressed transcripts among all sampling points in heart, skeletal muscle, and liver, respectively. There were few differentially expressed genes in common across all three tissues; these were enriched in mitochondrial and apoptotic pathway components. Divisive clustering of these data revealed unique cohorts of transcripts that increased across the torpor bout in each tissue with patterns reflecting various combinations of cycling within and between seasons as well as between torpor and arousal. Transcripts that increased across the torpor bout were likewise tissue specific. These data shed new light on the biochemical pathways that alter in concert with hibernation phenotype and provide a rich resource for further hypothesis-based studies.

Keywords Hibernation · Torpor · mRNA · Transcriptome · Liver · Heart · Skeletal muscle

Communicated by F. Breukelen.

This manuscript is part of the special issue Hibernation—Guest Editors: Frank van Breukelen and Jenifer C. Utz.

Electronic supplementary material The online version of this article (doi:10.1007/s00360-017-1073-x) contains supplementary material, which is available to authorized users.

✉ Lori K. Bogren
lori.bogren@ucdenver.edu

¹ Cell and Developmental Biology, University of Colorado School of Medicine, Aurora, USA

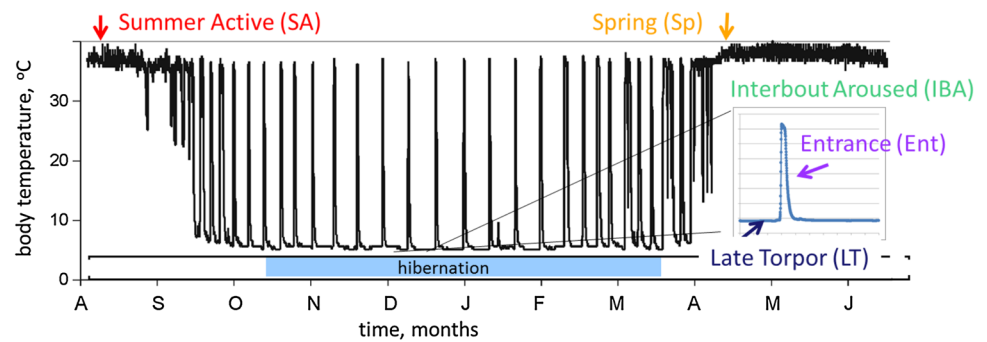
² Department of Genetics, Stanford University, Stanford, USA

³ HudsonAlpha Institute for Biotechnology, Huntsville, USA

Introduction

Small mammalian hibernators including the 13-lined ground squirrel (*Ictidomys tridecemlineatus*), spend winter in extended periods of torpor with drastic reductions in metabolic (3% BMR), heart (to 5–6 beats per min) and respiratory rates (to 3–4 breaths per min), and core body temperature (to Tb 2–10 °C) (Buck and Barnes 2000; Carey et al. 2003). All of these parameters are reversible and rapidly restored to euthermic levels using strictly endogenous mechanisms during short periods of interbout arousal, which occur every 10 days to 2 weeks (Fig. 1). Cycles between torpor and arousal are restricted to and persist throughout fall and winter; thus, hibernation is seasonal

Fig. 1 Precisely sampling points across the hibernator's year in relationship to body temperature and time. The hibernation season is delineated by the blue bar; hibernation sampling points are indicated in the offset showing the rapid arousal (LT to IBA) and entrance processes (IBA to Ent) for one torpor-arousal cycle



heterothermy. In contrast, these same animals remain homeothermic throughout spring and summer. Therefore, hibernation can be considered one phase of a seasonal cycle between homeothermy and heterothermy, with heterothermy being the result of repeated cycles between torpor and arousal (Epperson et al. 2011; van Breukelen and Martin 2015; Grabek et al. 2015). Other important cyclical behaviors that occur in concert with the seasonal cycle include reproduction, feeding, growth and fattening during the active phase, and cessation of feeding (i.e., prolonged fasting) during the hibernation phase. Neither the biochemical mechanisms orchestrating the switch between winter heterothermy and summer homeothermy, nor the switch between torpor and arousal, are fully understood; both are likely to be critical for successful hibernation.

Advances in the genomics of non-model organisms, particularly for mRNA and protein identification and quantification, have facilitated exploration into gene expression and transcript abundance changes in hibernators. Recently, transcriptome analyses using next-gen sequencing technologies have been performed on several tissues collected from distinct physiological states in 13-lined ground squirrels (Schwartz et al. 2013, 2015; Hampton et al. 2011, 2013; Vermillion et al. 2015a; Cooper et al. 2016; Grabek et al. 2015). However, the differences in sample timepoints, data collection, and analysis procedures among data sets make their comparison difficult (Conesa et al. 2016). Moreover, in some of these studies, limited sampling across the year and imprecision in the timing of sample collection (e.g., at an unknown time relative to Tb recovery during the short euthermic periods of hibernation) fail to accurately capture the complex dynamics of the hibernation phenotype (Fig. 1).

Recently, a BAT transcriptome analysis that used precisely collected physiological points across the circannual cycle revealed a subset of transcripts that increase in relative abundance over the torpor bout, likely due to selective mRNA stabilization (Grabek et al. 2015). The cohort of stabilized transcripts was enriched for gene products that are critical for non-shivering thermogenesis (e.g., lipolysis) which is needed for the earliest phases of rewarming as

the animals arouse from torpor (Grabek et al. 2015). Here we extend this analysis to three additional key metabolic organs, heart, skeletal muscle, and liver. The hindlimb muscles and liver are slow to perfuse during interbout arousal and thus slow to rewarm and recover their euthermic function, in contrast to BAT and heart which are perfused early during arousal and drive the rewarming process (Hampton et al. 2010; Schmidt-Nielsen 1997). We hypothesized that, similar to BAT, heart is likely to have a cohort of stabilized transcripts for immediate use in the early arousal period, while this cohort may not be evident in skeletal muscle and liver. Specifically, the goals of this study were to: (1) define and compare functional-group dynamics of the transcriptome in each of these organ systems; (2) determine whether cohorts of transcripts also increase during torpor at low Tb in organs other than BAT; and (3) if so, examine whether the stabilized transcripts are the same in all tissues or rather serve the unique function of their specific tissues. Overall, the purpose of the current study was not to single out specific gene dynamics but rather to consider the data more globally while making the individual gene findings available to the community as a hypothesis-generating tool.

Materials and methods

Animals and tissue collection

All animal procedures were performed in accordance with the Guide for the Care and Use of Laboratory Animals and approved by the University of Colorado Institutional Animal Use and Care Committee. Procurement and housing of the animals were as described (Grabek et al. 2015).

Tissues samples were collected from the heart, liver, and skeletal muscle (quadriceps) of animals representing five distinct physiological states in the circannual cycle based on date and Tb (Fig. 1). The two homeothermic (i.e., active or non-hibernating) states were spring (Sp, spring emerged as evidenced by a lack of torpor bouts for 6–39 days, Tb ~37°C, n=5 for skeletal muscle and liver, n=4 for heart) and summer active (SA, late July–early

August, $T_b=37^\circ\text{C}$, $n=5$ all tissues). The three heterothermic (i.e., hibernation) states were interbout aroused (IBA, $T_b=37^\circ\text{C}$ for 2–3 h after T_b crossed inflection point during rewarming, $n=5$ all tissues), entrance into torpor (Ent, $T_b=23\text{--}27^\circ\text{C}$, $n=5$ all tissues), and late torpor (LT, 80–95% of prior torpor bout duration, $T_b=4^\circ\text{C}$, $n=5$ all tissues). All animals were exsanguinated under isoflurane anesthesia, perfused with ice-cold saline, decapitated, and dissected on ice; tissues were immediately snap frozen in liquid nitrogen and stored at -80°C until RNA extraction.

EDGE-tag

Total RNA was extracted from the tissue samples using Trizol Reagent (Invitrogen). Quantity and quality of each RNA preparation were assessed by NanoDrop (Thermo Scientific) and Bioanalyzer (Agilent Technologies), respectively. Only samples with $\text{RIN} \geq 8.0$ were used for EDGE-tag library construction as previously described (Hong et al. 2011). Library preparation and sequencing was completed at the HudsonAlpha Institute of Biotechnology, Huntsville, AL, on the Illumina GAIIx (Illumina, San Diego, CA).

Data analysis

A series of in-house scripts were used to process the data for quantification. Off-sequencer reads were trimmed to the NlaIII site, and those longer than 20 nt were aligned first to the 13-lined ground squirrel mitochondrial genome [Fig. S1 in (Hampton et al. 2011)], and then to the genome (spetri2, Ensembl release 79) using bowtie (Langmead et al. 2009). Reads aligning uniquely to the genome were converted to bedgraph format and merged by genomic location (Quinlan and Hall 2010), and then annotated using the spectri2 gtf file (Ensembl release 79) with an in-house python script. Because most gene annotations in this species are limited to the protein-coding region, we defined tags that lie at or within 3000 nt downstream of the annotated 3' end of a gene as belonging to that gene.

Tag counts were converted to tags per million (TPM) with edgeR (Robinson et al. 2010). Poorly expressed tags were filtered, retaining only those with ≥ 2 TPM in $n-1$ samples in at least one sample group. Samples were then subjected to between-lane, nonlinear full quantile normalization using EDASeq (Risso et al. 2011). These data were used for clustering by Random Forest (Svetnik et al. 2003) in variable selection mode (Diaz-Uriarte 2007) with 100,000 initial trees, 50,000 subsequent forests, and dropping 20% of the remaining variables at each iteration to identify key separators (smallest number of tags giving the lowest out of box error) among the groups. These key tags were used to cluster the individual samples with 60,000 trees. The normalized EDGE-tag count data were also

used for differential expression (DE) analyses. Comparing all groups, the DE tags were identified using the negative binomial GLM in DESeq with no additional size factor normalization (Anders and Huber 2010) and p values were adjusted for multiple testing using the Benjamini–Hochberg false discovery rate correction. Pairwise significance and pairwise fold change between physiological states were calculated for all significant DE tags ($q < 0.05$) using DESeq. The DE tags within genes (≤ 3 kb from 3' end of gene annotations, called DE transcripts) were clustered by Divisive ANALysis (DIANA) to identify transcripts with shared dynamic patterns across all the sampling states. In some cases, there are multiple DE transcripts (i.e., multiple DE tags mapping within 3 kb of the 3' end of one gene); as a group these multiple DE transcripts from one gene are called DE genes. All DE, DIANA, and Random Forest analyses were conducted in R (R).

DAVID (Huang et al. 2009) was used for functional annotation and gene enrichment analysis of the various groups of DE genes including tissue specific, tissue shared, and DIANA clusters within tissues. Only those tags within 3 kb of a gene annotation (to assure reasonable confidence that the gene was correctly identified), i.e., DE transcripts, as listed for each tissue in Online Resource 1–3, DIANA tab, were used for gene enrichment analyses by DAVID. Top Gene Ontology terms for cell component, molecular function, and biological process were recovered using the chart option, while clusters with enrichment scores ≥ 1.3 and terms with Benjamini q value of ≤ 0.05 were considered significant in the analysis of the DIANA patterns for each tissue.

Results

Transcriptome dynamics in the heart, skeletal muscle, and liver were interrogated by sequencing 74 EDGE-tag libraries, representing five distinct physiological states across the circannual cycle: Sp and SA from the homeothermic period, and IBA, Ent, and LT from the hibernation period (Fig. 1). Approximately 90% of the reads (hereafter referred to as tags) in each tissue passed the initial filter (Online Resources 4). Of these, we found large differences in the mean fraction of reads across states that mapped to the mitochondrial genome, ranging from a high of 18 and 11% in heart and skeletal muscle, respectively, to a low of 3% in liver (Online Resource 4). In addition to these large tissue-specific differences, the relative abundance of tags representing mitochondrial DNA (mitochondrial transcripts) was state-dependent to a small extent in all three tissues: in heart, mitochondrial transcripts were elevated in LT compared to Sp by 1.5-fold; in skeletal muscle, they decreased in Sp ($\geq 1.6\times$) vs. all other groups; and in liver

they were highest in SA ($\geq 1.5\times$) compared to Sp, Ent, and LT. After filtering tags aligning to mitochondria, the remaining sequencing reads were mapped to the 13-lined ground squirrel genome where 55.8, 54.7, and 63.1% were uniquely aligned (Online Resources 4); only the subset of tags that were uniquely aligned to the genome are considered further here.

Random Forests clustering analysis

After filtering low abundance tags and library normalization (Table 1), supervised clustering of the data by Random Forest in variable selection mode revealed that a small subset of the tags could classify samples by physiological state in heart, skeletal muscle, and liver (Fig. 2). A unique set of best-classifying tags was identified for each tissue (Online Resources 1–3), with just eight needed to classify the heart samples with zero out-of-bag error, compared to 50 and 32 tags for skeletal muscle and liver, respectively. Importantly, the relationship of the different physiological states to one another based on these tag abundances differed substantially among the three tissues. In heart, Sp and Ent samples

were closest, with clear separation of SA, LT, and IBA. In skeletal muscle, the three groups with euthermic Tb clustered closely together (the homeothermic groups Sp and SA, plus IBA hibernators), with clear separation of the Ent and LT hibernators from the euthermic cluster and from one another. Finally, in liver, the Ent and LT hibernators (the two groups with lowering and lowest Tb, respectively) were juxtaposed but distinct from the three euthermic groups (Sp, SA, and IBA), which were also widely separated from one another. Although their proximities differed, the clear separation of the heterothermic states indicates that the transcriptome is dynamic across the torpor-arousal cycle in each tissue.

Differential expression, tissue comparisons

An independent analysis using DESeq (Anders and Huber 2010) identified 5572, 11,438, and 4198 tags that were differentially expressed among the five physiological states in heart, skeletal muscle, and liver, respectively ($q < 0.05$; Table 1). Simple quantification of pairwise differences in this subset of the data yields numbers broadly consistent

Table 1 Data filtering and analysis

	Heart	Skeletal muscle	Liver	Analysis
Starting tags	174,267	82,492	110,519	
After filtering ^a	30,048	25,339	25,627	Random forest
GLM significant (%) ^b	5572 (18.5)	11,438 (45.1)	4198 (16.4)	Pairwise comparisons
Within 3 kb ^c	3347	6784	2433	DIANA

^a ≥ 2 TPM in n-1 samples in at least one sample group

^b Percent significant ($q < 0.05$) post-filtered tags

^c Within 3 kb of the 3' end of a gene annotation

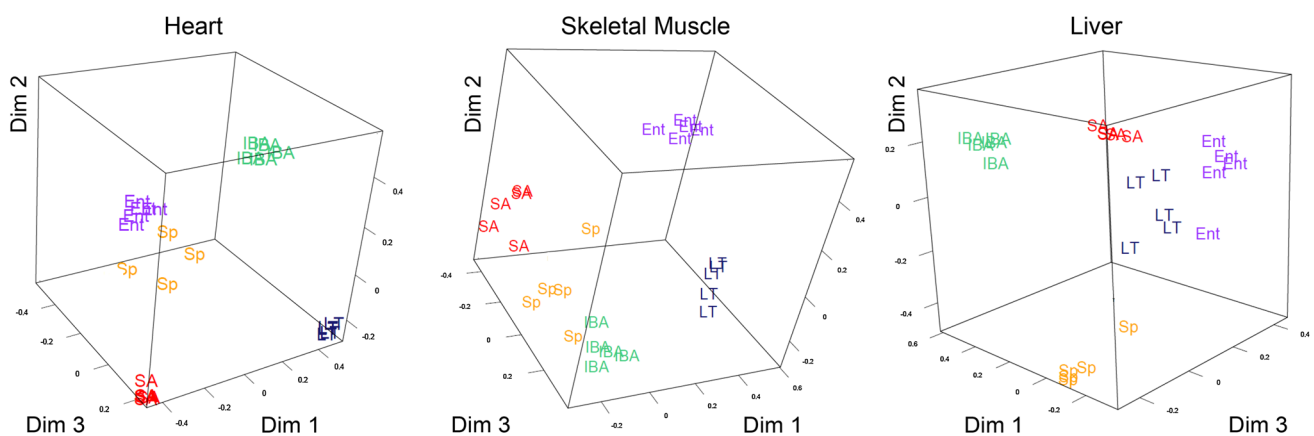


Fig. 2 The transcriptome of each tissue has a distinctive response during the circannual cycle. Three-dimensional scaling plots from supervised Random Forest using key EDGE-tag separators distinguish the transcriptomes of heart, skeletal muscle, and liver for the five physiological sampling points. The homeothermic phase of the

circannual cycle (Fig. 1) is represented by Spring (Sp) and Summer Active (SA); and Interbout Aroused (IBA), Entrance (Ent), and Late Torpor (LT) timepoints comprise the heterothermic (i.e., hibernation) phase. SA, Sp, and IBA animals share euthermic Tb

with the Random Forest results, in that each tissue responds differently with more or less evidence for distinct gene expression patterns among groups depending whether they are homeothermic or heterothermic, and if heterothermic, whether they are torpid, aroused from or re-entering torpor (Table 2). In heart and liver, the greatest number of DE tags occurred in pairwise comparisons between a homeothermic and heterothermic group (i.e., SA vs LT in heart; SA vs Ent in liver), whereas in skeletal muscle the most distinct pair occurred within hibernation (IBA vs Ent), consistent with each tissue forming a distinct grouping pattern by Random Forest. Gene enrichment analysis, using just the subset of DE tags that were also within 3 kb of the nearest gene, revealed that the DE transcripts in each tissue were enriched for functions consistent with expectations for that tissue. For example, the top three Biological Process GOterms were: muscle contraction, muscle system process, and muscle organ development in heart; protein catabolism, ATPase activity coupled to movement of substances, and muscle organ development in skeletal muscle; and oxidation reduction, carboxylic acid biosynthesis, and steroid biosynthesis in liver.

The DE gene lists from the three tissues were examined for overlaps to determine the degree to which the same genes were differentially expressed in the different tissues (Fig. 3, Online Resource 5). Not surprisingly given their common mesodermal origin, heart and skeletal muscle shared the greatest number of DE genes, 988, compared to just 158 in heart and liver, and 388 in skeletal muscle and liver. The common DE genes in heart and skeletal muscle were enriched for muscle-specific cellular components including contractile fiber, myofibril, and sarcomere as well as muscle organ development and macromolecular catabolism including proteolysis. In contrast, DE genes common to liver and heart were not significantly enriched for any function or cell component, and those common to liver and skeletal muscle were only enriched in endoplasmic reticulum. The top enrichment categories of the 389 genes that were DE in all three tissues were mitochondrion and apoptosis.

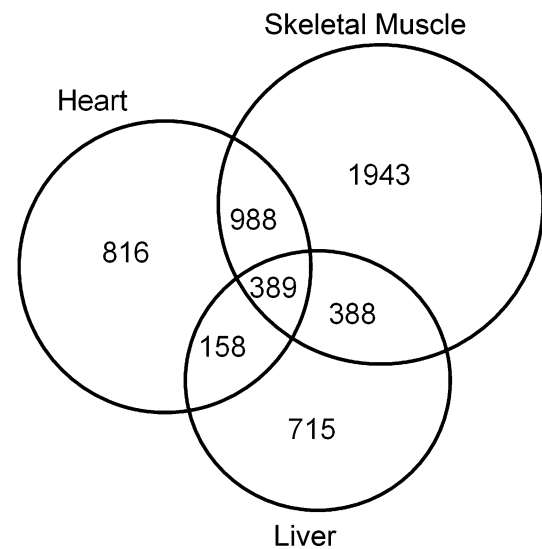


Fig. 3 Venn diagram. Each tissue is represented by a circle; the number of differentially expressed EDGE-tags (GLM, $q < 0.05$, within 3 kb of a gene annotation) that are unique or shared among the three tissues is indicated

Dynamic patterns and their functional annotations

Next, we grouped the DE transcripts (EDGE-tags mapping within 3 kb of 3' ends of annotated genes) in each tissue into clusters, based on their shared relative abundance dynamics across the five physiological states, using the divisive clustering algorithm, DIANA. Each cluster was subsequently analyzed for functional enrichment. Eight of the 12 heart DIANA clusters had significant functional annotation enrichments based on DAVID analysis, as did 8 of 9 of the skeletal muscle, and 6 of the 12 liver DIANA clusters (Figs. 4, 5, 6).

The DIANA pattern with the greatest number of DE transcripts in the heart also exhibited the greatest number of informative annotations. Cluster 1 had 820 DE transcripts with greater relative abundance in heterotherms (Ent, IBA and LT hibernators) than in homeotherms (Sp and SA). These were also dynamic in the torpor-arousal

Table 2 Pairwise differential expression

	Heart					Skeletal muscle					Liver				
	Sp	SA	IBA	Ent	LT	Sp	SA	IBA	Ent	LT	Sp	SA	IBA	Ent	LT
Sp	–					–					–				
SA	183	–				1696	–				679	–			
IBA	220	208	–			485	2912	–			233	459	–		
Ent	418	447	124	–		2517	81	3275	–		118	694	66	–	
LT	1288	1400	342	56	–	428	950	505	814	–	47	127	127	115	–

Number of differentially expressed tags across the circannual cycle in the heart, skeletal muscle, and liver. Pairwise comparisons were conducted in DESeq using GLM significant tags ($q < 0.05$). Each tissue showed a unique pair of states with the greatest number of DE tags

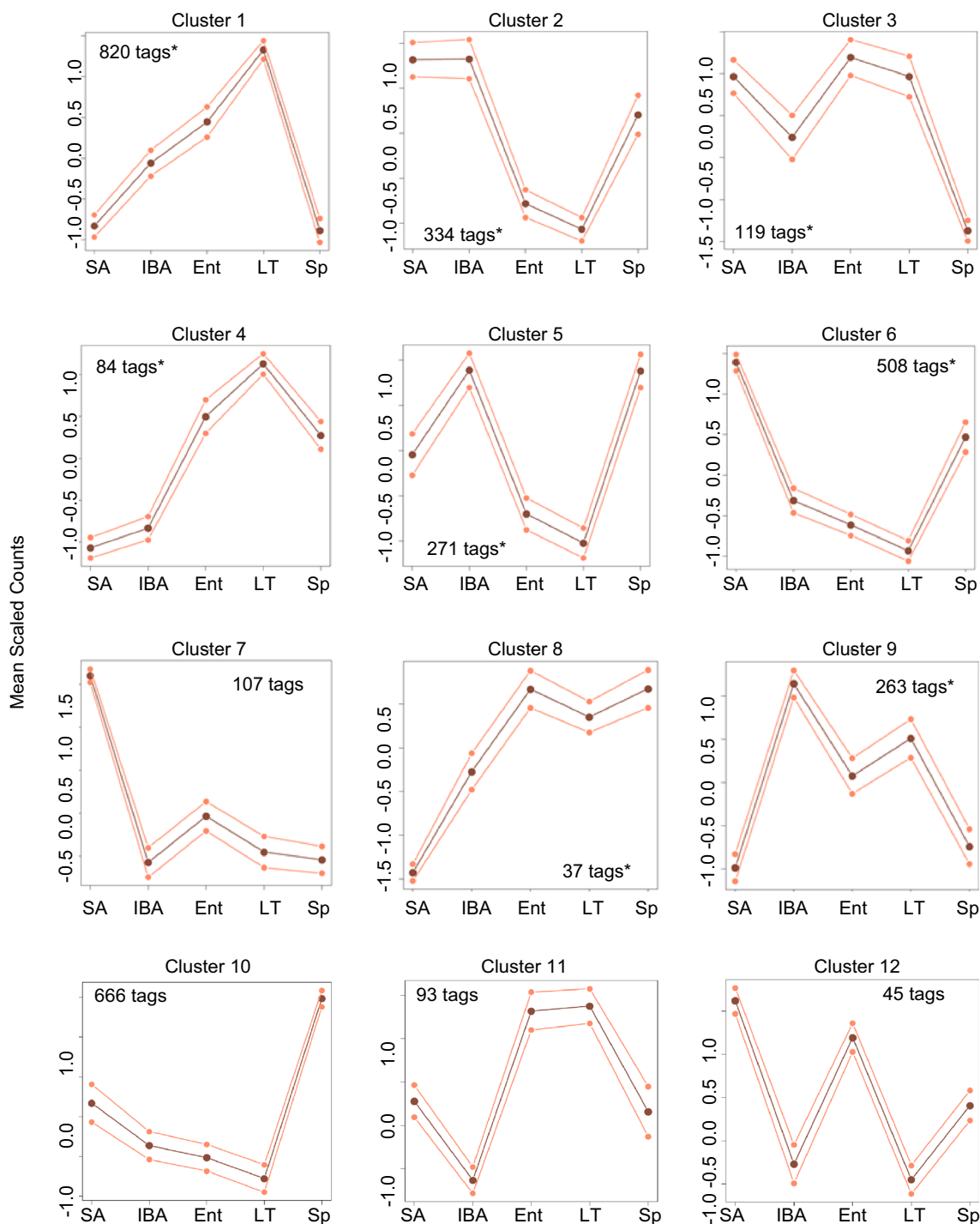


Fig. 4 In the heart, DIANA analysis of all GLM significant tags ($q < 0.05$) within 3000 nt of an annotated gene yielded 12 patterns of transcript abundance dynamics over the circannual cycle; mean scaled counts (brown line) \pm sem (orange lines). Number of tags in

each cluster is indicated. Asterisks denote clusters which contained genes that yielded significantly enriched annotations (enrichment score ≥ 1.3 ; $q \leq 0.05$) via DAVID analysis

cycle, reaching their greatest abundance in LT (Fig. 4). The DE genes in this cluster were enriched for several unique functional annotations, including protein catabolism, proteasome and ubiquitin ligase, peroxisome, and

beta oxidation. Additionally, they were enriched in contractile fiber and sarcomere, functional annotation enrichments shared with clusters 2 and 3, despite their distinct dynamic patterns. Another noteworthy pattern was found in cluster

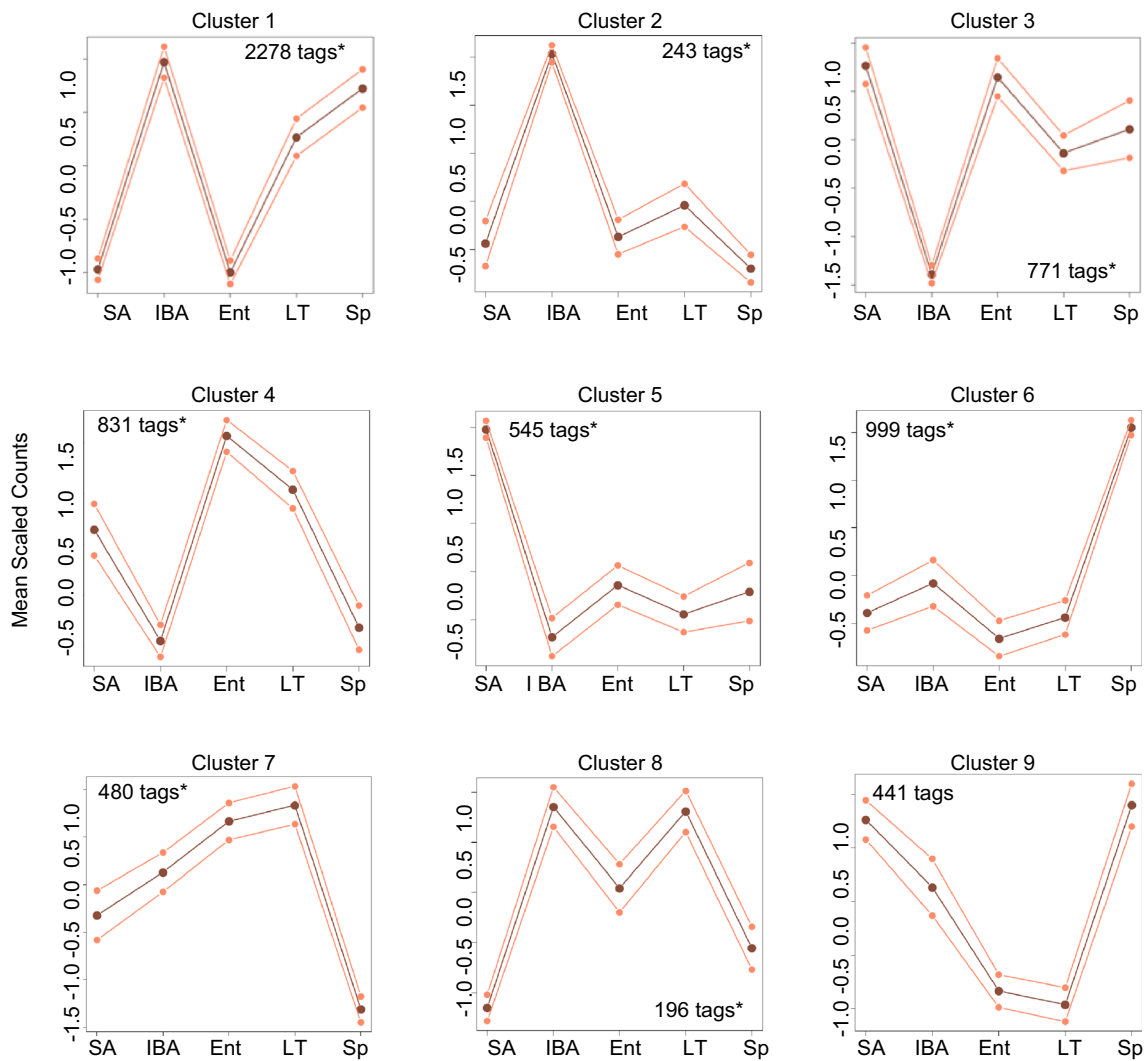


Fig. 5 Over the circannual cycle, skeletal muscle had nine dynamic patterns of transcript abundances for tags that were GLM significant and within 3000 nt of an annotated gene; mean scaled counts (*brown line*) ± sem (*orange lines*). Number of tags in each cluster is given.

Clusters comprised of genes that contained significantly enriched annotations from DAVID analysis (enrichment score ≥ 1.3 ; $q \leq 0.05$) are indicated by an *asterisk*

4 in which the relative DE transcript abundance was greatest in Ent, LT, and Sp, but low in SA and IBA. This pattern is enriched for fibrillar collagen and extracellular matrix. Finally, two DIANA patterns that shared the property of having the lowest DE transcript abundance during Ent and LT, the two lowest Tb timepoints in this study (clusters 2 and 5), were enriched for genes involved in transcriptional regulation and transcriptional enhancers.

In skeletal muscle, the dynamic pattern with the greatest number of DE transcripts (2278 DE genes) was cluster 1 (Fig. 5). The DE transcripts in this cluster reached their greatest relative abundance during IBA and low abundance during SA and Ent. This pattern was unique to skeletal muscle (i.e., a similar dynamic pattern was not observed in heart or liver) and enriched for a large number of DE

genes that form muscle structures as well as those functioning in protein catabolism. There were also enrichments of DE genes involved in positive regulation of transcription, ubiquitin-associated translation elongation, and phosphorous, glucose and acetyl-CoA metabolic processes in cluster 1. The related pattern in DIANA cluster 2 is likewise enriched for contractile fiber components but also contains cell-substrate junction components. Two patterns that were effectively the reciprocals of these, i.e., their abundance is lowest in IBA, clusters 3 and 4, were also enriched for DE genes that function in protein catabolism (cluster 3), and contractile fiber components (cluster 4), with the additional enrichments of amino acid ligase activity and protein localization in cluster 3, and mitochondrial envelope in cluster 4. DE genes involved in muscle tissue development were

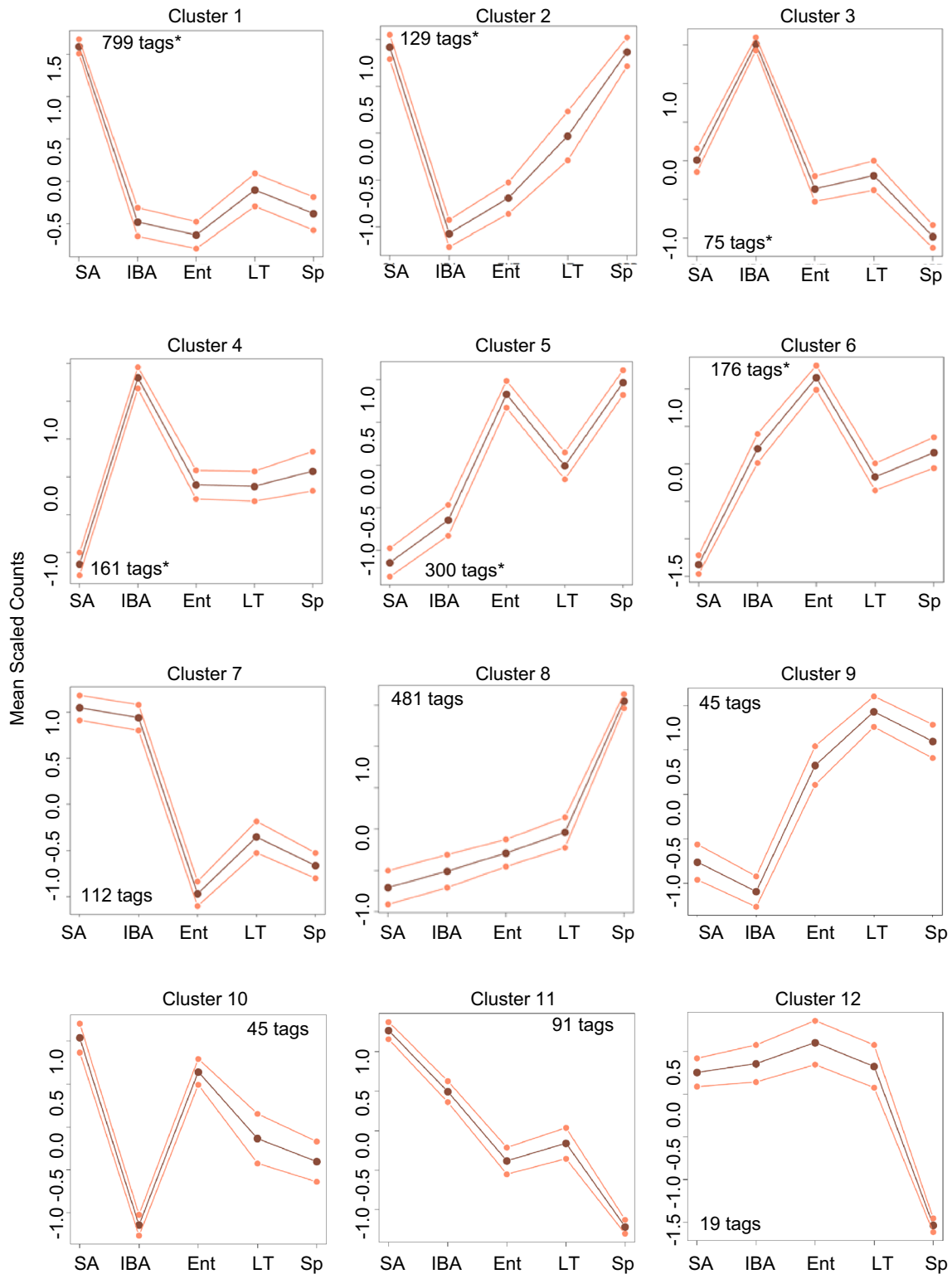


Fig. 6 DE EDGE-tags in the liver (GLM $q < 0.05$, within 3000 nt of an annotated gene) were clustered into 12 dynamic patterns of transcript abundance over the circannual cycle. Number of tags in each cluster is given. Six clusters contained genes yielding significantly

enriched annotations (enrichment score ≥ 1.3 ; $q \leq 0.05$) via DAVID analysis and are denoted with an asterisk; mean scaled counts (brown line) \pm sem (orange lines)

enriched in the cluster with highest relative abundance in summer (SA, cluster 5), where structural components of muscle (contractile fiber, sarcomere) and focal adhesion proteins are also enriched. Cluster 6 was comprised of a large number of DE transcripts that are relatively increased during spring (Sp); these DE genes were enriched for additional components of the contractile fiber and sarcomere as well as protein catabolic process and extracellular matrix. The DE transcripts comprising cluster 7 are lowest in Sp, elevated during hibernation, and enriched for mitochondrial membrane components. Cluster 8 DE transcripts were also elevated throughout hibernation, but were lowest in SA. This cluster was enriched for mitochondrial outer membrane components. Cluster 9 had no enriched functional annotation clusters.

Twelve dynamic patterns were found for the liver DE genes, but just six of these had significant DAVID functional annotation clusters (clusters 1–6, Fig. 6 and Online Resource 3). The cluster with the greatest number of DE transcripts, 799, had a dynamic pattern with highest abundance in summer (SA) compared to low abundance in the other states, despite modest dynamics in hibernation (cluster 1). Cluster 1 DE genes were enriched for glucose and triglyceride metabolic processes, lysosome and polygenic dyslipidemia, urea cycle, nicotinamide metabolic processes, and vitamin B6 binding. The only other cluster with high DE transcript abundance in SA that also contained significant functional annotation enrichments was cluster 2 (129 DE transcripts), where the DE transcripts were abundant in both of the homeothermic states, SA and Sp, but low in IBA, and then increased between Ent and LT hibernators. The DE genes in cluster 2 were enriched for function in hexose metabolic processes and alcohol biosynthesis. Clusters 3 and 4 (75 and 161 DE transcripts, respectively) peaked during IBA. Two heat shock protein groups were enriched in cluster 3, chaperone Hsp70 and its co-chaperone, DnaJ. Cluster 4 had only one significant annotation, organelle lumens. Finally, clusters 5 (300 DE transcripts) and 6 (176 DE transcripts) were lowest in SA and highest in Ent. The functional enrichments peroxisome (cluster 5), tRNA aminoacylation, and monocarboxylic acid transport (both cluster 6) were found in these clusters.

Transcripts increasing in relative abundance during a torpor bout

Finally, we examined the DIANA clusters for patterns with DE transcripts that increased in their relative abundance during a torpor bout, i.e., after several days at low Tb when transcription does not occur (van Breukelen and Martin 2002) and increased abundance is thus likely due to selective preservation of some transcripts from degradation across the torpor bout (Grabek et al. 2015). Transcripts

were considered to increase over a torpor bout if the mean scaled counts of the DIANA pattern were higher in LT compared with Ent and the sem of these two timepoints did not overlap. DE transcripts that increased across the torpor bout were found in all three tissues, specifically: clusters 1, 4, and 9 in heart; clusters 1 and 8 in skeletal muscle, and clusters 1, 2, 7, and 9 in liver (Figs. 4, 5, 6). The significant functional enrichments of the DE genes in these clusters were described above.

Discussion

Understanding how the transcriptome changes in various tissues in concert with the hibernator's dramatic physiological transitions is an important first step toward elucidating the molecular underpinnings of the hibernation phenotype. In the current study, we employed a common data collection and analysis pipeline using a high-throughput sequencing approach to compare transcriptome dynamics across five physiologically distinct timepoints in the circannual cycle among three tissue types. These timepoints capture both the seasonal and torpor-arousal cycles of hibernation in the 13-lined ground squirrel. Microarray analysis of differential gene expression, which has been used to study hibernation, is limited by the genes on the chip, a problem for non-model organisms like hibernators. In contrast, the EDGE-tag method used here has no such limitation but instead relies on alignment with the annotated genome (White and Salamonsen 2005; Hong et al. 2011). For heart, skeletal muscle and liver, we sought to identify both shared and unique patterns of transcriptome dynamics associated with the hibernation phenotype, and specifically whether and which transcripts increased after at least one week in torpor at low Tb. We found that these three tissues responded largely uniquely, with different sensitivities to season and Tb, and in accordance with their tissue-specific functions. We further found that while there are dynamic patterns containing groups of transcripts that increase in relative abundance across the torpor bout in all three tissues, these transcripts are for the most part tissue specific.

The first indication of the uniqueness of transcriptome dynamics in heart, skeletal muscle, and liver appeared during the initial step of data analysis, i.e., during mapping the EDGE-tag reads to mitochondrial DNA. We found large differences in the fraction of reads that mapped to the mitochondrial genome, ranging from a high of 18 and 11% in heart and skeletal muscle, respectively, to a low of 3% in liver (Online Resource 4), consistent with previous report for the two muscles (Hampton et al. 2011), and with the known importance of oxidative metabolism in the heart (Andrews et al. 2009; Vermillion et al. 2015b). The fraction of mitochondrial reads was also relatively stable in heart,

but more dynamic in skeletal muscle and liver, each with a distinct pattern. In skeletal muscle, mitochondrial reads were lowest in Sp, consistent with the switch to increased reliance on glucose compared to fatty acid fuels as the animals begin feeding after their long winter fast (Hindle et al. 2011; Carey et al. 2003). In liver, mitochondrial reads were highest in SA compared to all other timepoints, coinciding with the period of fattening, where excess fuel is converted in liver to fatty acids for storage in white adipose tissue (Lanaspa et al. 2015; Serkova et al. 2007; South and House 1967).

Further indication of the uniqueness of the transcriptome dynamics in each of these three tissues appears in the clustering of the five physiological states as defined by Random Forest analysis based on the relative abundance counts from the genome-mapped EDGE-tags. The best separation of physiological states occurred with a distinct subset of tags, and the clustering patterns of the five states relative to one another were unique for each tissue type (Fig. 2). In contrast to plasma metabolomics (Epperson et al. 2011) and heart (Grabek et al. 2011), skeletal muscle (Hindle et al. 2015), and liver (Hindle et al. 2014) proteomic analyses, where Random Forest clusters homeotherms distinct from heterotherms, the EDGE-tags clustered at least one of the homeothermic groups closer to a heterothermic group (e.g., Sp and Ent in heart, IBA and Sp in skeletal muscle, and SA and all the hibernator groups in liver) than to the other homothermic group (e.g., SA or Sp). While some of these differences in the classification of hibernation states based on metabolites, proteins and transcripts may be attributed to the use of additional physiological groups in the metabolomic and proteomic analyses, it is likely that the far greater depth of the transcriptome and the lack of one-to-one correspondence between the transcriptome and the proteome (Vermillion et al. 2015b; Vogel and Marcotte 2012) also contribute. Nonetheless, it is clear that the subset of the transcriptome that classifies individuals based on physiological state is unique to each tissue.

The relative abundance patterns of the DE transcripts and their gene enrichments as determined by the DIANA clustering and DAVID analysis of those clusters also differed substantially among the three tissues (Figs. 4, 5, 6). In heart the dynamic cluster with the greatest number of DE genes and functional annotations had increased DE transcript abundance seasonally for hibernation, but then also increased from IBA to Ent to LT within the torpor-arousal cycle (Cluster 1, Fig. 4). In contrast, the dynamic pattern with the greatest number of genes in skeletal muscle had low abundance during SA and Ent, and was highest in IBA, but also elevated in LT and Sp. Thus the genes in this group were dynamic in and among both homeotherms and heterotherms (Cluster 1, Fig. 5). In liver, the majority of the DE transcripts cycled little during hibernation (although they

exhibited a modest but significant increase from Ent to LT; Cluster 1, Fig. 6), but were highest in SA and low in Sp, so again they differed in and among both homeotherms and heterotherms. When considered in light of shared dynamic patterns there were no common functional enrichment categories across tissues. Furthermore, many of the identified DE genes do not appear in any of the functional enrichment clusters and many are not usefully identified (Gene name ensembl, Online Resources 1–3). Therefore, a substantial number of DE genes are excluded from the enrichment analysis. While the highlighted functional enrichments provide substantial biological insight into pathways altered in hibernation, there is a great deal more to be learned from these data. This is particularly true regarding the DE genes that fall outside of the known enrichment clusters, which are not based on knowledge of hibernators. Overall, these complex and diverse transcriptome dynamics highlight the importance of careful sampling in multiple tissues across both the seasonal and torpor-arousal cycles of hibernation in order to gain a molecular understanding of this complex phenotype.

The heart amplifies its function nearly a 100-fold from the torpid rate of 5 to 400 beats per minute during arousal from torpor (Hampton et al. 2010). This rapid activation may be supported by the relative increase in glycolytic and beta oxidation related gene products over the torpor bout (Cluster 1, Fig. 4) and by the apparent remodeling of the contractile and supporting structures in the heart both seasonally and within hibernation (Clusters 1–3, Fig. 4). These results add important features to the growing pool of heart transcriptome data for hibernating animals, including: (1) rigorous criteria to define sample collection timepoints based on continuous Tb data obtained from implanted devices; (2) three collection times during hibernation Ent, LT, and IBA rather than just torpor and euthermic; and (3) a greater separation of the homeothermic states from the heterothermic states, compared to previous work using high-throughput sequencing technologies to quantify transcriptome dynamics in 13-lined ground squirrel heart (Hampton et al. 2011; Vermillion et al. 2015a, b). One of these earlier studies found that fetal genes are activated during the hibernation season (Vermillion et al. 2015a). This is significant because the cardiac fetal gene program is also activated in adults under pathophysiological conditions, including hypertrophy, hypoxia, and ischemia (Taegtmeier et al. 2010; Kuwahara 2013). Of the fetal genes reported previously (NKX2.5, NFATc1, MEF2A, GATA4, MYOCD, and TBX20), our DE gene set captured only NFATc1 and MEF2A. NFATc1 appeared in cluster 2 along with 49 other genes involved in transcription. This pattern was highly dynamic in hibernators, cycling from highest abundance in IBA, to low in Ent and lowest in LT. MEF2A was found in both clusters 1 and 9, where the DE transcripts are

seasonally elevated in hibernation and also dynamic across the torpor-arousal cycle. Its appearance in these two clusters with different dynamics in hibernation would be consistent with two isoforms of this transcript having distinct regulation. The question of transcript isoform regulation across hibernation states remains to be examined.

Some of the discrepancies among the present 13-lined ground squirrel transcriptome analysis and those in earlier studies (Hampton et al. 2011; Vermillion et al. 2015a, b) are no doubt attributable to the sampling differences, but some are also likely due to the method of gene annotation. In the earlier work, a transcriptome was assembled *de novo* and used for transcript quantification, whereas in the present study we used the Ensembl genome for the 13-lined ground squirrel and corresponding annotations to map and identify genes. It is worth mentioning here that “ensembl” appears numerous times as a gene ID in all of our tables. This annotation is given for any gene for which an unidentified open reading frame has been identified by homology; further identification may be possible based on the corresponding genome coordinates in the supporting tables. However, consistent with an activation of fetal gene expression, our results lend further support to the view that the heart is not completely protected from stress during hibernation (Vermillion et al. 2015a). The terms for fibrillar collagen and extracellular matrix were significantly enriched in Cluster 4. Here, gene expression increased in entrance and was highest by late torpor. This pattern of increased relative expression during low Tb is consistent with enhanced stabilization of these transcripts so that they may be quickly translated during arousal, when the heart must function in conditions analogous to an ischemia–reperfusion environment. Coupled with increased fetal gene expression, our results suggest that production of collagen may serve to quickly repair areas of experiencing cardiomyocyte death that occurs during this period of acute stress (Dobaczewski et al. 2012). Interestingly, the term for apoptosis was significantly enriched in Cluster 2, where transcript abundance increased during interbout arousal relative to the other heterothermic groups. Further study is now needed to follow the dynamics of cell death, proliferation and collagen production in the heart throughout hibernation.

A comparison of these transcript data with proteomic data collected from similar samples in heart also reveals differences in the two datasets. Clustering analysis using proteomic data found that five identified proteins were best able to separate individuals into their respective states (Grabek et al. 2011). There was no overlap between these proteins (CFL2, Cofilin 2; HSPA4, Heat Shock 70 kDa Protein 4; DBT, dihydrolipoyl transacylase; APOA1, Apolipoprotein A1; and TTR, Transthyretin) and the transcripts that separated the groups in the current data. This may be explained in part by post-translational mechanisms: the

variance in CFL2 expression resulted from changes in its phosphorylation state and not total protein expression. Furthermore, the proteomic data captured proteins that likely originated outside of the cell, such as the plasma transport proteins APOA1 and TTR. Finally, while only 432 protein “spots” were previously analyzed, our transcriptome analysis included 30,048 tags, resulting in a much broader view of the gene products expressed at each sampling point. Likewise, there was no overlap between the protein and transcript functional annotations identified as significant during specific periods of the circannual cycle. A discrepancy between transcriptome and proteome was also seen in data from a recent proteogenomic analysis (Vermillion et al. 2015b). This previous study found MYL2 and MYL7 proteins were downregulated during hibernation. Yet in our dataset, the transcripts for these two proteins were the two most abundant in the combined winter groups. Overall, these data illuminate the likelihood that additional regulatory mechanisms dissociate transcription and translation product abundances across the phenotypic transitions of the hibernator’s year (Biggar and Storey 2015).

Skeletal muscle findings were unique in several ways from the other two tissues in this study: this tissue had the greatest number of DE tags (11,438) by more than a factor of two with the largest number of pairwise differences (3275) separating two hibernation states, IBA vs Ent; in the Random Forest analysis, skeletal muscle transcripts exhibited relative juxtaposition of all of the warm Tb animals, whether from homeothermic or heterothermic seasons; finally, there were three DIANA clusters in skeletal muscle with the unique pattern of large tag abundance changes from IBA to both SA and Ent which were similar to each other.

There is a growing but incomplete understanding of the molecular mechanisms behind the role of skeletal muscle in the physiological transitions in the circannual cycle and also the hibernator’s ability to retain muscle mass over the hibernation season, despite extended disuse (Hindle et al. 2015; Bogren et al. 2016). Several of the dynamic patterns in our dataset were enriched with various sarcomere and contractile fiber components, indicating both active season (clusters 1, 5, and 6, Fig. 5) and torpor-arousal cycle dependent (clusters 1 and 2, Fig. 5) remodeling of these critical muscle components. Some of these patterns are nearly reciprocal of one another (compare cluster 1 to cluster 4 in Fig. 5) as are patterns with enrichments of protein catabolism (cluster 1 vs cluster 3, Fig. 5). These reciprocal patterns suggest important regulatory differences; their DE genes should be examined in hypothesis-driven experiments for their role in muscle remodeling and rebuilding across the long period of inactivity—a property of hibernator muscle that is at least in part attributable to increased translation and rebuilding toward the end of the hibernation

season (Hindle et al. 2015; Bogren et al. 2016), although the critical molecular components are unknown. A recent proteogenomics study reported that the largest differences in protein abundances occur between March and April, but these were mainly changes in metabolic enzymes (Anderson et al. 2016). In our study, metabolic enzymes were enriched in Cluster 1 (Fig. 5), which cycled rapidly from a high in the aroused hibernator (IBA) to a low as the animals reentered torpor (Ent), approximately 12 h later. The tags in cluster 1 were also elevated in the spring homeotherms, consistent with this also being an active muscle remodeling and rebuilding phase.

Liver

This is the first multistate transcriptome analysis for the liver using high-throughput sequencing methods in a hibernating ground squirrel species. The liver transcriptome showed both seasonal and Tb effects on the clustering of these five physiological states by Random Forest, a property which is also apparent in the DIANA clusters. These findings, as with the other tissues examined, differ from previously published findings from similar studies of the proteome. The dominant cycle in the proteome was seasonal and was highly enriched for metabolic enzymes that distinguished feeding (homeothermic, active season) from fasting (heterotherms) animals (Hindle et al. 2014). At the transcriptome level, the metabolic enzymes were concentrated in cluster 1 (Fig. 6), where transcript abundance is highest in SA, and low in all other states including Sp. This likely reflects the important role of the liver in converting all excess energy gained through feeding during the pre-hibernation fattening period (i.e., SA) to storage fat for the long winter fast.

Previous work has shown that, even during the low temperatures of torpor, some transcripts are stabilized and increased in relative abundance while most are slowly degraded (Grabek et al. 2015). Thus, the time elapsed at the time of collection since entry into a torpor period could greatly influence the relative abundance of transcripts. Likewise, transcripts can only be resynthesized when Tb increases during the periodic arousals from torpor, and the timing of their transcription across the euthermic period may greatly affect relative abundance. Indeed each of the tissues exhibit DIANA patterns that have both steep increases and steep decreases when IBA is compared to Ent or LT timepoints among the hibernation states. As with BAT, heart, skeletal muscle and liver all have cohorts of transcripts that increase during the torpor phase of hibernation, i.e., exhibit increased abundance between Ent and LT. Rather than being a constant set of genes that are selected for protection from degradation during torpor, each tissue appears to stabilize its own tissue-specific transcripts

across the torpor bout. The majority of these with low fold change (i.e., less than twofold) likely represent inherently more stable transcripts compared to the total pool (Grabek et al. 2015).

Conclusion

Using identical data processing pipelines together with samples collected within precise physiological and temporal parameters, we compared the hibernators changing transcriptome in the heart, skeletal muscle, and liver. Our study highlights a unique transcriptome response with distinct biochemical implications over the circannual cycle for each tissue but with the commonality of metabolic pathway transcript abundances being prioritized to persist over a torpor bout. These findings point to new lines of investigation to decipher tissue-specific mechanisms that may contribute to, or potentially play a role in regulating the transition between homeothermy and heterothermy or the switch into or out of torpor. However, further work is needed to determine the key components and relative importance of transcription, RNA processing and stability in supporting various aspects of the hibernation phenotype. Our data clearly indicate that progress regarding our understanding of how the ground squirrel genome orchestrates the hibernation phenotype will depend on studies of gene expression that use carefully collected, precisely timed samples in a multitude of tissues throughout the body.

Acknowledgements The tissue bank was collected with the support of NIH HL-089049 and the sequencing data by HudsonAlpha. The data analysis pipeline was developed in part to fulfill course requirements of the Genomics workshop at the University of Colorado Anschutz Medical Campus and benefited greatly from the help of Drs. S. Peach and J. Hesselberth, as well as from insights gleaned from an earlier analysis by Dr. C. Henegar, then at HudsonAlpha.

References

- Anders S, Huber W (2010) Differential expression analysis for sequence count data. *Genome Biol* 11(10):R106. doi:10.1186/gb-2010-11-10-r106
- Anderson KJ, Vermillion KL, Jagtap P, Johnson JE, Griffin TJ, Andrews MT (2016) Proteogenomic analysis of a hibernating mammal indicates contribution of skeletal muscle physiology to the hibernation phenotype. *J Proteome Res* 15(4):1253–1261. doi:10.1021/acs.jproteome.5b01138
- Andrews MT, Russeth KP, Drewes LR, Henry PG (2009) Adaptive mechanisms regulate preferred utilization of ketones in the heart and brain of a hibernating mammal during arousal from torpor. *Am J Physiol Regul Integr Comp Physiol* 296(2):R383–R393. doi:10.1152/ajpregu.90795.2008
- Biggar KK, Storey KB (2015) Insight into post-transcriptional gene regulation: stress-responsive microRNAs and their role in the

- environmental stress survival of tolerant animals. *J Exp Biol* 218 (Pt 9):1281–1289. doi:[10.1242/jeb.104828](https://doi.org/10.1242/jeb.104828)
- Bogren LK, Johnston EL, Barati Z, Martin PA, Wojda SJ, Van Tets IG, LeBlanc AD, Donahue SW, Drew KL (2016) The effects of hibernation and forced disuse (neurectomy) on bone properties in arctic ground squirrels. *Physiol Rep* 4 (10). doi:[10.14814/phy2.12771](https://doi.org/10.14814/phy2.12771)
- Buck CL, Barnes BM (2000) Effects of ambient temperature on metabolic rate, respiratory quotient, and torpor in an arctic hibernator. *Am J Physiol Regul Integr Comp Physiol* 279(1):R255–R262
- Carey HV, Andrews MT, Martin SL (2003) Mammalian hibernation: cellular and molecular responses to depressed metabolism and low temperature. *Physiol Rev* 83(4):1153–1181. doi:[10.1152/physrev.00008](https://doi.org/10.1152/physrev.00008)
- Conesa A, Madrigal P, Tarazona S, Gomez-Cabrero D, Cervera A, McPherson A, Szcześniak MW, Gaffney DJ, Elo LL, Zhang X, Mortazavi A (2016) A survey of best practices for RNA-seq data analysis. *Genome Biol* 17:13. doi:[10.1186/s13059-016-0881-8](https://doi.org/10.1186/s13059-016-0881-8)
- Cooper ST, Sell SS, Fahrenkrog M, Wilkinson K, Howard DR, Bergen H, Cruz E, Cash SE, Andrews MT, Hampton M (2016) Effects of hibernation on bone marrow transcriptome in thirteen-lined ground squirrels. *Physiol Genom* 48(7):513–525. doi:[10.1152/physiolgenomics.00120.2015](https://doi.org/10.1152/physiolgenomics.00120.2015)
- Diaz-Uriarte R (2007) GeneSrf and varSelRF: a web-based tool and R package for gene selection and classification using random forest. *BMC Bioinform* 8:328. doi:[10.1186/1471-2105-8-328](https://doi.org/10.1186/1471-2105-8-328)
- Dobaczewski M, de Haan JJ, Frangogiannis NG (2012) The extracellular matrix modulates fibroblast phenotype and function in the infarcted myocardium. *J Cardiovasc Transl Res* 5(6):837–847. doi:[10.1007/s12265-012-9406-3](https://doi.org/10.1007/s12265-012-9406-3)
- Huang DW, Sherman BT, Lempicki RA (2009) Systematic and integrative analysis of large gene lists using DAVID bioinformatics resources. *Nat Protoc* 4(1):44–57. doi:[10.1038/nprot.2008.211](https://doi.org/10.1038/nprot.2008.211)
- Epperson LE, Karimpour-Fard A, Hunter LE, Martin SL (2011) Metabolic cycles in a circannual hibernator. *Physiol Genom* 43(13):799–807. doi:[10.1152/physiolgenomics.00028.2011](https://doi.org/10.1152/physiolgenomics.00028.2011)
- Grabek KR, Karimpour-Fard A, Epperson LE, Hindle A, Hunter LE, Martin SL (2011) Multistate proteomics analysis reveals novel strategies used by a hibernator to precondition the heart and conserve ATP for winter heterothermy. *Physiol Genom* 43(22):1263–1275. doi:[10.1152/physiolgenomics.00125.2011](https://doi.org/10.1152/physiolgenomics.00125.2011)
- Grabek KR, Diniz Behn C, Barsh GS, Hesselberth JR, Martin SL (2015) Enhanced stability and polyadenylation of select mRNAs support rapid thermogenesis in the brown fat of a hibernator. *Elife* 4:e04517. doi:[10.7554/eLife.04517](https://doi.org/10.7554/eLife.04517)
- Hampton M, Nelson BT, Andrews MT (2010) Circulation and metabolic rates in a natural hibernator: an integrative physiological model. *Am J Physiol Regul Integr Comp Physiol* 299(6):R1478–R1488. doi:[10.1152/ajpregu.00273.2010](https://doi.org/10.1152/ajpregu.00273.2010)
- Hampton M, Melvin RG, Kendall AH, Kirkpatrick BR, Peterson N, Andrews MT (2011) Deep sequencing the transcriptome reveals seasonal adaptive mechanisms in a hibernating mammal. *PLoS One* 6(10):e27021. doi:[10.1371/journal.pone.0027021](https://doi.org/10.1371/journal.pone.0027021)
- Hampton M, Melvin RG, Andrews MT (2013) Transcriptomic analysis of brown adipose tissue across the physiological extremes of natural hibernation. *PLoS One* 8(12):e85157. doi:[10.1371/journal.pone.0085157](https://doi.org/10.1371/journal.pone.0085157)
- Hindle AG, Karimpour-Fard A, Epperson LE, Hunter LE, Martin SL (2011) Skeletal muscle proteomics: carbohydrate metabolism oscillates with seasonal and torpor-arousal physiology of hibernation. *Am J Physiol Regul Integr Comp Physiol* 301(5):R1440–R1452. doi:[10.1152/ajpregu.00298.2011](https://doi.org/10.1152/ajpregu.00298.2011)
- Hindle AG, Grabek KR, Epperson LE, Karimpour-Fard A, Martin SL (2014) Metabolic changes associated with the long winter fast dominate the liver proteome in 13-lined ground squirrels. *Physiol Genom* 46(10):348–361. doi:[10.1152/physiolgenomics.00190.2013](https://doi.org/10.1152/physiolgenomics.00190.2013)
- Hindle AG, Otis JP, Epperson LE, Hornberger TA, Goodman CA, Carey HV, Martin SL (2015) Prioritization of skeletal muscle growth for emergence from hibernation. *J Exp Biol* 218 (Pt 2):276–284. doi:[10.1242/jeb.109512](https://doi.org/10.1242/jeb.109512)
- Hong LZ, Li J, Schmidt-Küntzel A, Warren WC, Barsh GS (2011) Digital gene expression for non-model organisms. *Genome Res* 21(11):1905–1915. doi:[10.1101/gr.122135.111](https://doi.org/10.1101/gr.122135.111)
- Kuwahara K (2013) Role of NRSF/REST in the regulation of cardiac gene expression and function. *Circ J* 77(11):2682–2686
- Lanaspá MA, Epperson LE, Li N, Cicerchi C, Garcia GE, Roncal-Jimenez CA, Trostel J, Jain S, Mant CT, Rivard CJ, Ishimoto T, Shimada M, Sanchez-Lozada LG, Nakagawa T, Jani A, Stenvinkel P, Martin SL, Johnson RJ (2015) Opposing activity changes in AMP deaminase and AMP-activated protein kinase in the hibernating ground squirrel. *PLoS One* 10(4):e0123509. doi:[10.1371/journal.pone.0123509](https://doi.org/10.1371/journal.pone.0123509)
- Langmead B, Trapnell C, Pop M, Salzberg SL (2009) Ultrafast and memory-efficient alignment of short DNA sequences to the human genome. *Genome Biol* 10(3):R25. doi:[10.1186/gb-2009-10-3-r25](https://doi.org/10.1186/gb-2009-10-3-r25)
- Quinlan AR, Hall IM (2010) BEDTools: a flexible suite of utilities for comparing genomic features. *Bioinformatics* 26(6):841–842. doi:[10.1093/bioinformatics/btq033](https://doi.org/10.1093/bioinformatics/btq033)
- R <http://cran.r-project.org>. <http://cran.r-project.org>
- Risso D, Schwartz K, Sherlock G, Dudoit S (2011) GC-content normalization for RNA-Seq data. *BMC Bioinform* 12:480. doi:[10.1186/1471-2105-12-480](https://doi.org/10.1186/1471-2105-12-480)
- Robinson MD, McCarthy DJ, Smyth GK (2010) edgeR: a Bioconductor package for differential expression analysis of digital gene expression data. *Bioinformatics* 26(1):139–140. doi:[10.1093/bioinformatics/btp616](https://doi.org/10.1093/bioinformatics/btp616)
- Schmidt-Nielsen K (1997) Animal physiology: adaptation and environment. Cambridge University Press, Cambridge, UK
- Schwartz C, Hampton M, Andrews MT (2013) Seasonal and regional differences in gene expression in the brain of a hibernating mammal. *PLoS One* 8(3):e58427. doi:[10.1371/journal.pone.0058427](https://doi.org/10.1371/journal.pone.0058427)
- Schwartz C, Hampton M, Andrews MT (2015) Hypothalamic gene expression underlying pre-hibernation satiety. *Genes Brain Behav* 14(3):310–318. doi:[10.1111/gbb.12199](https://doi.org/10.1111/gbb.12199)
- Serkova NJ, Rose JC, Epperson LE, Carey HV, Martin SL (2007) Quantitative analysis of liver metabolites in three stages of the circannual hibernation cycle in 13-lined ground squirrels by NMR. *Physiol Genom* 31(1):15–24. doi:[10.1152/physiolgenomics.00028.2007](https://doi.org/10.1152/physiolgenomics.00028.2007)
- South FE, House WA (1967) Energy metabolism in hibernation. In: Mammalian hibernation III. Oliver & Boyd, Edinburgh
- Svetnik V, Liaw A, Tong C, Culbertson JC, Sheridan RP, Feuston BP (2003) Random forest: a classification and regression tool for compound classification and QSAR modeling. *J Chem Inf Comput Sci* 43(6):1947–1958. doi:[10.1021/ci034160g](https://doi.org/10.1021/ci034160g)
- Taetgen H, Sen S, Vela D (2010) Return to the fetal gene program: a suggested metabolic link to gene expression in the heart. *Ann N Y Acad Sci* 1188:191–198. doi:[10.1111/j.1749-6632.2009.05100.x](https://doi.org/10.1111/j.1749-6632.2009.05100.x)
- van Breukelen F, Martin SL (2002) Reversible depression of transcription during hibernation. *J Comp Physiol B* 172(5):355–361. doi:[10.1007/s00360-002-0256-1](https://doi.org/10.1007/s00360-002-0256-1)
- van Breukelen F, Martin SL (2015) The hibernation continuum: physiological and molecular aspects of metabolic plasticity in mammals. *Physiology* (Bethesda, Md) 30(4):273–281. doi:[10.1152/physiol.00010.2015](https://doi.org/10.1152/physiol.00010.2015)
- Vermillion KL, Anderson KJ, Hampton M, Andrews MT (2015a) Gene expression changes controlling distinct adaptations in the

- heart and skeletal muscle of a hibernating mammal. *Physiol Genom* 47(3):58–74. doi:[10.1152/physiolgenomics.00108.2014](https://doi.org/10.1152/physiolgenomics.00108.2014)
- Vermillion KL, Jagtap P, Johnson JE, Griffin TJ, Andrews MT (2015b) Characterizing cardiac molecular mechanisms of mammalian hibernation via quantitative proteogenomics. *J Proteome Res* 14(11):4792–4804. doi:[10.1021/acs.jproteome.5b00575](https://doi.org/10.1021/acs.jproteome.5b00575)
- Vogel C, Marcotte EM (2012) Insights into the regulation of protein abundance from proteomic and transcriptomic analyses. *Nat Rev Genet* 13(4):227–232. doi:[10.1038/nrg3185](https://doi.org/10.1038/nrg3185)
- White CA, Salamonsen LA (2005) A guide to issues in microarray analysis: application to endometrial biology. *Reproduction* 130(1):1–13. doi:[10.1530/rep.1.00685](https://doi.org/10.1530/rep.1.00685)